Journal of Macromolecular Science, Part A
Publication details, including instructions for authors and subscription information:
http://www.informaworld.com/smpp/title~content=t713597274

Pyrolysis Kinetics of a Polyurethane Foam by Thermogravimetry; A General Kinetic Method

F. E. Rogers[a]; T. J. Ohlemiller[a]
[a] Mechanical and Aerospace Engineering Department, Princeton University, Princeton, New Jersey

To cite this Article Rogers, F. E. and Ohlemiller, T. J.(1981) 'Pyrolysis Kinetics of a Polyurethane Foam by Thermogravimetry; A General Kinetic Method', Journal of Macromolecular Science, Part A, 15: 1, 169 — 185
To link to this Article: DOI: 10.1080/00222338108066438
URL: http://dx.doi.org/10.1080/00222338108066438

J. MACROMOL. SCI.–CHEM., A15(1), pp. 169-185 (1981)

Pyrolysis Kinetics of a Polyurethane Foam by Thermogravimetry; A General Kinetic Method

F. E. ROGERS and T. J. OHLEMILLER

Mechanical and Aerospace Engineering Department
Princeton University
Princeton, New Jersey 08544

ABSTRACT

Kinetic studies on the decomposition of a flexible polyurethane foam based on tolylene diisocyanate and a polyether polyol of propylene oxide have been carried out with the thermogravimetric technique (TGA). In dry nitrogen the decomposition proceeds in two overall steps. At the end of the first step, which follows a diffusion-controlled rate law, the cellular structure collapses to a viscid liquid. The viscid liquid decomposes further in accord with a random nucleation rate law. The activation parameters which provide very good fits to the experimental TGA curves at heating rates of 2 and 20°/min are $A_1 = 3.4 \times 10^{19}$ min^{-1}, $E_1 = 52$ kcal/mole, and $A_2 = 6.8 \times 10^{12}$ min^{-1}, $E_2 = 39$ kcal/mole. A general approach for the derivation of kinetic parameters for such complex reactions is presented.

INTRODUCTION

In connection with a study of the smoldering combustion of polyurethane foams [1-7], it became necessary to develop procedures to evaluate the overall kinetics of the decomposition of these materials. This communication deals with the decomposition kinetics of a particular flexible foam which exhibits a marked smolder tendency.

Commercial flexible polyurethane foams are most often prepared from tolylene diisocyanate (TDI, 80:20 mixture of 2,4- and 2,6-isomers), a polyether polyol, water, a blowing agent, catalysts, and a surfactant. The principal bonds formed in the polymerization reaction are urethane and urea groups.

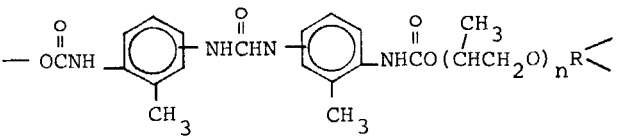

The urea bonds are formed in a hydrolysis-addition reaction sequence between water and two isocyanate groups [8].

Several recent investigations show the product distribution and discuss the mechanistic aspects of the thermal decomposition of polyurethanes [9, 10]. The urethane is clearly the most thermolabile bond. Woolley found that at low temperatures (200 to 300°C) there was a rapid and complete loss of tolylene diisocyanate from a TDI-propylene oxide (PPO) polymer as a yellow smoke leaving a polyol residue [10]. A carbon-14 tracer study on the thermal decomposition of a similar foam at 207°C shows that some TDI is retained in carbodiimide formation [11].

The kinetics of the thermal decomposition of polyurethanes has received less systematic attention. Isothermal studies on the thermal degradation of a linear polyurethane in vacuum at 260 to 300°C indicated a diffusion-controlled, random chain-scission process with an activation energy of 14.1 kcal/mole [12]. Nonisothermal studies on the decomposition of a flexible polyurethane (TDI-PPO) in dry nitrogen show a dependence of the kinetics on molecular weight of the polyol. As the molecular weight of the polyol increases from ~300 to 2700, the activation energy and reaction order decrease from 36.2 kcal/mole and 0.72 to 25.9 kcal/mole and 0.26 [13]. For model linear polyurethanes from xylylenediisocyanate and dimethylolcyclohexane, the mechanism and kinetics of thermal decomposition have been established. The derived activation energy varied from 20 to 32 kcal/mole depending on the calculation method and the experimental technique employed [14].

EXPERIMENTAL

Materials

The foam used in this study was prepared from an 80:20 TDI mixture and a trifunctional polyol according to the recipe given in Table 1.

TABLE 1. Flexible Urethane Foam

Formulation	Parts by weight
Propoxylated triol (3000 MW)	100
Water	5.0
Silicone surfactant (L-540)[a]	1
Bis-dimethylaminoethyl ether (Al)[a]	0.1
Stannous octoate	0.30
Tolylene diisocyanate (80:20 mixture of 2,4/2,6-isomers)	59.9

[a]Union Carbide Corp.

Apparatus

For the pyrolysis studies reported here, measurements of weight loss on a mass fraction-remaining basis vs temperature were obtained using the DuPont 951 Thermogravimetric Analyzer (TGA) as part of the DuPont 990 Thermal Analysis System. In using the DuPont 990 System several operational features were noted which have a significant influence on calculated kinetics. First, the nominal heating rates indicated on the instrument generally were lower than the actual experimental heating rates measured during the course of an experiment. Second, although the instrument simultaneously plots the time derivative of the weight loss curve, it was observed to be inaccurate at nominal heating rates exceeding 10°C/min. In the present method the DTG curve was used only for diagnostic purposes; however, in other work on the pyrolysis kinetics of cellulose it assumed a more important role and a computer approach to the calculation of each DTG curve was developed [15]. Third, strong temperature gradients were observed along the length of the TGA furnace. Since the "sample" thermocouple also senses the local furnace temperature, the penetration distance, within the furnace, of the quartz tube containing the sample pan and sample thermocouple was observed to affect weight loss vs temperature results. This distance was set so that the melting points of aluminum, tin, and zinc fell within the accuracy of the type K thermocouple used in the DuPont system.

For experiments reported here, small samples (1.5 to 1.8 mg) of foam were introduced into the platinum sample pan and the instrument was subsequently purged for 1 hr using flowing dry nitrogen (50 mL/min) to reduce the concentration of oxygen within the system to below detectable limits. The sample was then dried to constant weight at 110°C and heated to 650°C in the flowing nitrogen at nominal heating rates of 2, 5, 10, and 20°/min.

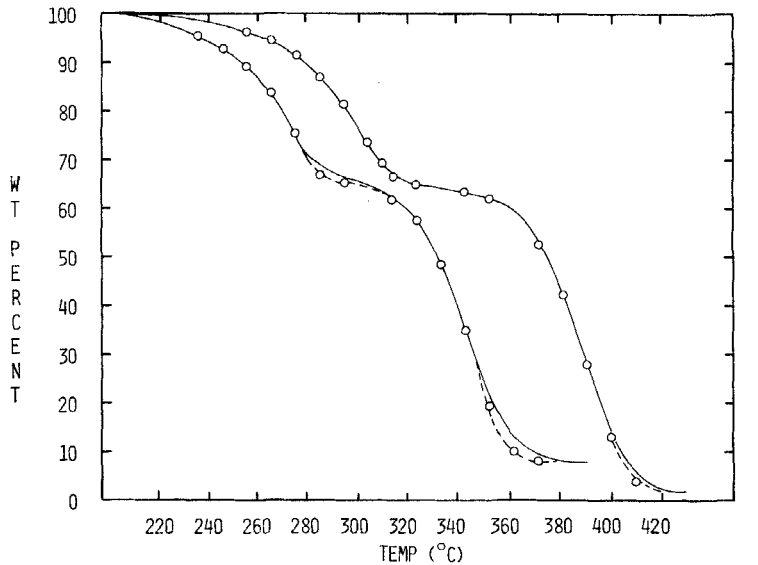

FIG. 1. Comparison of experimental (—) and theoretical (○) TGA curves for the thermal decomposition of a flexible polyurethane foam at experimental heating rates of 2.15 and 22.3°/min using rate laws and kinetic parameters given in text.

RESULTS AND DISCUSSION

The TGA curves for the thermal decomposition of the flexible urethane foam is nitrogen at 2 and 20°C/min are shown in Fig. 1. The decomposition takes place in two overall steps and the completion of the first step transforms the cellular structure to a tarry, viscous liquid. In describing this sequence of events, our purpose is to derive those kinetic parameters which provide the best fit to the entire experimental curve at both heating rates. In this way we are assured of an empirical description of the decomposition process at heating rates comparable to those found in smoldering combustion and thus suitable for mathematical model development [3, 6].

General Kinetic Method

The derivation of kinetic data from TGA curves obtained under nonisothermal conditions has received considerable attention and several comprehensive reviews are available [16-18]. In general, the kinetic procedure consists of three parts: the choice of a suitable heterogenous reaction mechanism, the calculation of the apparent

kinetic parameters for this rate law, and finally the testing of the kinetics description against the experimental data at several heating rates.

At present, there are some 16 laws in existence to explain heterogenous reactions of the type found in polymer degradation [19-22]. These rate laws are divided into four groups: (1) diffusion, (2) phase boundary reaction, (3) random nucleation, and (4) power laws. All these laws have as their starting point the generalized rate equation

$$\frac{da}{dT} = \frac{k}{\beta} f(a) \tag{1}$$

where β = linear heating rate, a = fraction reacted, $k = Ae^{-E/RT}$, and f(a) is the particular rate law in question. Also, the integral of da/f(a) is customarily called g(a) so that

$$\int \frac{da}{f(a)} = g(a) = \frac{A}{\beta} \int e^{-E/RT}\, dT \tag{2}$$

The g(a)'s for the 16 rate laws are given in Table 2.

The evaluation of the right-hand integral in Eq. (2) has been more troublesome and several approximate solutions have appeared in the literature [23-25]:

$$\frac{A}{\beta} \int e^{-E/RT}\, dT \simeq \frac{ART^2/E}{(1 + 4RT/E)^{1/2}} \cdot e^{-E/RT} \qquad \text{[Ref. 25]}$$

$$\simeq \frac{A}{\beta}\left(1 - \frac{2RT}{E}\right)\frac{RT^2}{E} \cdot e^{-E/RT} \qquad \text{[Ref. 23]}$$

$$\simeq \frac{ART^2}{\beta(E + 2RT)} e^{-E/RT} \qquad \text{[Ref. 24]}$$

We have compared each approximation with a theoretical curve obtained from a fourth-order Runge-Kutta integration routine. Using the following kinetic parameters, we derived two numerical curves and compared the three approximate solutions in Table 3: E = 30 kcal/mole, $A = 4.2 \times 10^{11}$ min^{-1}, n = 1 (random nucleation), $\beta = 5°/min$ and E = 45 kcal/mole, $A = 6 \times 10^{14}$ min^{-1}, n = 1, $\beta = 5°/min$. (These kinetic parameters cover thermal decomposition reactions in the

TABLE 2. Rate Laws for Heterogenous Reactions

Model (symbol)		g(a)	
1) Diffusion	(D1)	a^2	Parabolic law; 1-D diffusion
	(D2)	$(1 - a) \ln (1 - a) + a$	2-D diffusion; cylindrical geometry
	(D3)	$[1 - (1 - a)^{1/3}]^2$	3-D diffusion; spherical geometry
	(D4)	$(1 - 2a/3) - (1 - a)^{2/3}$	3-D diffusion; spherical geometry
2) Phase boundary reactions (B)		$[1 - (1 - a)^n]$	n = 1/2, 1/3
3) Random nucleation (R)		$[-\ln (1 - a)]^n$	n = 1, 2/3, 1/2, 1/3, 1/4
4) Power laws (P)		a^n	n = 1/4, 1/3, 1/2, 1, 3/2

TABLE 3. Comparison of Integral Approximations

Kinetic parameters: $A = 4.2 \times 10^{11}$ min^{-1}, E = 30 kcal/mole, R(1) model, B = 5°C/min

	Mass fraction			
T (°C)	Runge-Kutta[a]	Coats and Redfern [23]	Gorbachev [24]	Balarin [25]
200	0.9840	0.9839	0.9839	0.9839
210	0.9681	0.9679	0.9678	0.9677
220	0.9383	0.9381	0.9378	0.9377
230	0.8854	0.8850	0.8846	0.8843
240	0.7969	0.7964	0.7956	0.7952
250	0.6611	0.6606	0.6593	0.6587
260	0.4782	0.4776	0.4759	0.4751
270	0.2756	0.2753	0.2735	0.2727

(continued)

TABLE 3 (continued)

Kinetic parameters: $A = 4.2 \times 10^{11}$ min^{-1}, E = 30 kcal/mole, R(1) model, B = 5°C/min

	Mass fraction			
T(°C)	Runge-Kutta[a]	Coats and Redfern [23]	Gorbachev [24]	Balarin [25]
280	0.1100	0.1099	0.1086	0.1081
290	0.0244	0.0245	0.0240	0.0237
$\sum \left\lvert \frac{(\text{RK-Approx})}{\text{RK}} \right\rvert \left(\frac{1}{n}\right)$	= .10%		0.48%	0.71%

Kinetic parameters: $A = 6 \times 10^{14}$ min^{-1}, E = 45 kcal/mole, R(1) model, B = 5°C/min

	Mass fraction			
T(°C)	Runge-Kutta[a]	Coats and Redfern [23]	Gorbachev [24]	Balarin [25]
300	0.9887	0.9886	0.9886	0.9886
310	0.9772	0.9770	0.9770	0.9769
320	0.9551	0.9548	0.9548	0.9546
330	0.9144	0.9139	0.9137	0.9136
340	0.8432	0.8425	0.8420	0.8418
350	0.7273	0.7261	0.7254	0.7251
360	0.5580	0.5566	0.5555	0.5551
370	0.3502	0.3487	0.3476	0.3470
380	0.1566	0.1555	0.1546	0.1541
390	0.0399	0.0394	0.0390	0.0388
$\sum \left\lvert \frac{(\text{RK-Approx})}{\text{RK}} \right\rvert \left(\frac{1}{n}\right)$	= 0.30%		0.53%	0.64%

[a]A fourth-order Runge-Kutta integration routine was used.

temperature range of 200 to 400°C.) The accuracy of each approximation is within the reproducibility of the TGA curves obtained with the present instrument. Each approximation is of comparable accuracy for the high temperature reaction and the Coats-Redfern equation [23] is slightly better for the low temperature reaction. Using the Gorbachev approximation, the generalized form of the rate law is therefore

$$g(a) = \frac{ART^2}{\beta(E + 2RT)} \cdot e^{-E/RT} \tag{3}$$

where g(a) is any one of the 16 tabulated functions (Table 2).

Criado [26] has provided a simple method for an easy and quick analysis of the apparent mechanism of thermal decomposition reactions of solids from DTG curves. This method does not pinpoint which of the 16 rate laws is the most appropriate, but it does simplify the process significantly. The Criado method is based on a series of master curves that depend neither on the kinetic parameters nor on the heating rate, but only on the reaction mechanism. Each master curve is obtained from a plot of the "reduced rate" against a, the former term being defined as

$$(T/T_{0.5})^2(da/dt)/(da/dt)_{0.5}$$

Here the subscript denotes the value at a = 0.5 and $(T/T_{0.5})^2$ is close to unity, so the "reduced rate" is approximated by the ratio of the rates or the ratio of the distances of the DTG curve from the base line. The master curves for various mechanisms are close together up to a = 0.5, then diverge, showing the greatest difference in the vicinity of a = 0.75. The maxima of these curves also show a shift which has diagnostic utility. In Table 4 we have tabulated the "reduced rate" at a = 0.75 and 0.80 for each of the 16 mechanisms shown in Table 2. Also shown in this table are the values of a at the "reduced rate" maximum and the expected ratio of apparent activation energies (E_a) for unresolved cases within particular sets of mechanisms. For example, if the "reduced rate" at a = 0.75 is 1 and the maximum occurs at a = 0.63, then any one of five random nucleation mechanisms with n = 1/4, 1/3, 1/2, 2/3, or 1 is suggested. However, each of these five rate laws requires different apparent activation energies whose values will be in the ratio shown in the last column. What this means, for example, is that an experimental TGA curve might be equally well fit with either the R(1) or R(1/2) law, but the E_a of the R(1/2) solution will be 1/2 that of the E_a for the R(1) solution. This situation is illustrated in Fig. 2 which shows two theoretical TGA curves that are nearly coincidental (maximum difference is

TABLE 4. Dependence of Reduced Reaction Rate on Fraction Reacted and on Reaction Mechanism

	Reduced rate			
Symbol (n)[a]	a = 0.75	a = 0.80	(a) at maximum	Ratio of E_a [b]
R(1/4), R(1/3), R(1/2), R(2/3), R(1)	1.00	0.93	0.63	1:1.3:2:2.7:4
D3, B(1/3)	1.13	1.09	0.70	1:1.9
B(1/2)	1.21	1.19	0.75	
D4	1.24	1.24	0.77	
D2	1.31	1.34	0.83	
P(1/4), P(1/3), P(1/2), P1, P(3/2), D1	1.5	1.6	1.0	1:1.3:2:4:6:8

[a]Symbols from Table 1.

[b]Expected ratio of apparent activation energies for the order listed in Column 1. The approximate ratio of the apparent activation energies for the first member of the groups listed in Column 1; i.e., R(1/4), D3, B(1/2), D4, D2, P(1/4), is 1:8:4:8:8:1 [19].

1.5%) even though the two sets of kinetic parameters chosen have E_a of 15 and 30 kcal/mole. The last column of Table 4 further suggests that it is possible to obtain a solution within the experimental reproducibility of a TGA curve with an E_a as low as 7.5 kcal/mole. Therefore, unless the DTG curves suggest one of the unambiguous rate laws (B(1/2), D4, or D2), it is impossible to obtain a unique set of kinetic parameters from a single TGA curve. This nonuniqueness of kinetic parameters for a single curve may help explain the great variation of activation energy parameters reported in the literature, especially when E_a alone or only E_a and A are given.

The most suitable set of kinetic parameters may be established by using a second nonisothermal curve or a nonisothermal and an isothermal curve combination [22]. The use of two or more different nonisothermal curves to derive activation energy is called the multiple heating rate method [27] and is based on the assumption that the temperature displacement between two or more curves at a point of equal conversion is a function of the activation energy. Procedural factors (sample size and weight, particle size, atmosphere) are also known to affect the temperature shift of TGA curves, especially in reversible reactions which show a greater sensitivity to diffusional factors

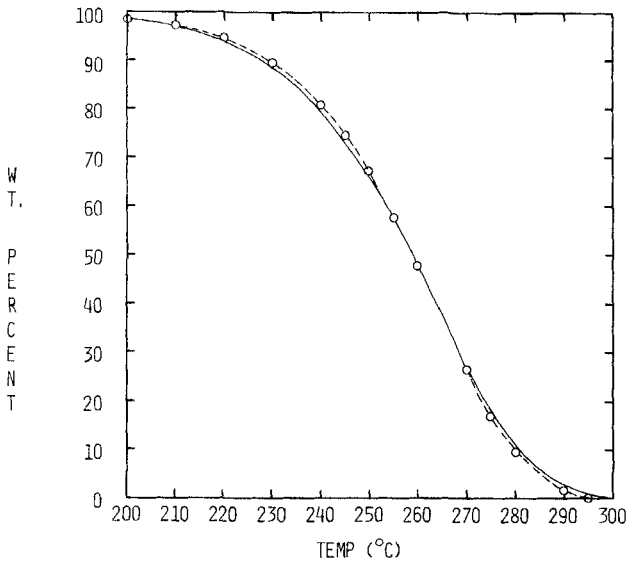

FIG. 2. Theoretical TGA curves obtained with kinetic parameters: $A = 4.2 \times 10^{11}$ min^{-1}, E = 30 kcal/mole, R(1) Model (—); $A = 1.84 \times 10^{5}$ min^{-1}, E = 15 kcal/mole, R(1/2) Model (○). At low and high conversion, curves differ by only 1 to 1.5%.

[28, 29]. Also, the value of the apparent activation energy will depend on the precision of the measured temperature difference. Thus a 2°C error in a typical temperature shift of 20 to 30°C introduces a 5 to 10% error in E_a. At the beginning and end of a reaction the temperature changes very rapidly with conversion so it is better to evaluate the temperature shift in the central portion (~ 90 to 10% range) of the decomposition. Using small samples (2 to 3 mg) and identical experimental procedures, we have found the multiple heating rate method to be a useful diagnostic tool in deriving a very good formal kinetic description for the irreversible decomposition of cellulose in steam at heating rates of 5 to 150°/min [15]. In the present work we reduced the sample weight further (1.7 ± 0.1 mg) and have again employed this method as a diagnostic aid in establishing the proper mechanism.

Unfortunately, the thermal decomposition of a polymeric material seldom proceeds according to a single, well-defined mechanism. More often, the degradative pathway is a series of complex steps made up of competitive, independent, and/or consecutive reactions. Furthermore, the reaction steps in these three sequences may proceed by different rate laws. This situation becomes very complex if the steps in the reactions overlap appreciably. General methods for extracting

the mechanism and rate parameters for such TGA curves are not available, and one is left with what amounts to trial and error integrations of possible rate schemes in attempting to match the experimental data. There is no guarantee of uniqueness in the parameter set that one finds to give a best fit so that conclusions about mechanisms are not justifiable.

In the following, we assume that the various reaction steps are unambiguously separated (or can be separated by proper choice of heating rate). Then the individual steps can be analyzed as if they comprise an entire TGA curve. Afterwards, one generates the full multistep TGA curve to check against the experimental curve. Even here restrictions enter in and analytical expressions cannot be given for all possible cases. Below we give expressions for simple competitive, independent, and consecutive reactions which can be used with Eq. (3) and a graphic relationship between the g(a) function and (a) to calculate a theoretical curve; this is then compared with the experimental trace.

The simplest competitive reaction case is

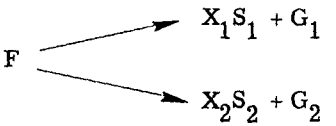

where $X_{1(2)}$ is the mass fraction of solid 1(2) left ungasified at the end of the reaction. Letting $X = X_1 + X_2$, mass conservation leads to the following expression for the TGA curve:

$$\frac{W_T}{W_O} = [1 - a(1 - X)] \qquad (4)$$

where W_T = sample weight at T, W_O = original sample weight, and (a) comes from $g(a) = G_1 + G_2$ (when the two reactions follow the same mechanism). G_1 and G_2 are the Gorbachev approximations for reaction (1) and (2) (Eq. 3). Here (a) is the fraction of original F consumed by both pathways.

For two independent reactions of the type

$$A = \delta F \longrightarrow X_1S_1 + G_1$$

$$B = (1 - \delta)F \longrightarrow X_2S_2 + G_2$$

Fraction δ of the fuel behaves as Material A; the remainder as Material B. $X_{1(2)}$ is the mass fraction of solid 1(2) left ungasified at the end of the reaction. Mass conservation gives the following equation for the TGA curve of such independent reactions:

$$\frac{W_T}{W_0} = \delta[1 - a_1(1 - X_1)] + (1 - \delta)[1 - a_2(1 - X_2)] \tag{5}$$

where $a_{1(2)}$ is the mass fraction of component 1(2) reacted. The values of $a_{1(2)}$ are obtained as in the single reaction case since the reactions here do not interact.

For the simple case of two consecutive reactions of the type

$$F \longrightarrow X_1 S_1 + G_1$$

$$S_1 \longrightarrow X_2 S_2 + G_2$$

the expression below for the TGA curve applies:

$$\frac{W_T}{W_0} = \left(1 - a_1\left(1 - X_1\left(1 - a_2(1 - X_2)\right)\right)\right) \tag{6}$$

Here the fractions reacted are obtained using Eq. (3) for the original fuel F and for the intermediate S_1; note that an accurate value of X_1 can only be obtained with reasonably separated reactions. Here we note that the final weight fraction is $X_1 X_2$.

Consecutive and independent reactions often behave similarly with regard to changes in heating rate so a distinction between the two modes may often not be possible. Using the same set of kinetic parameters that have been used elsewhere [16, 27] to illustrate the difference in behavior of competitive and independent reactions, we have plotted the TGA curves for consecutive and independent reactions in Fig. 3. This figure shows that these closely coupled reactions converge as the heating rate is increased for both modes of reaction. At 0.5°/min, where the reactions are somewhat separated, the consecutive and independent TGA curves are almost identical. At 2°/min, small differences begin to appear in the central position of the DTG curves and grow at 5°/min. At 5°/min the TGA curve for the consecutive mode is displaced to higher temperature by several degrees so that at 460°C, about 2 to 3% less sample is converted. In

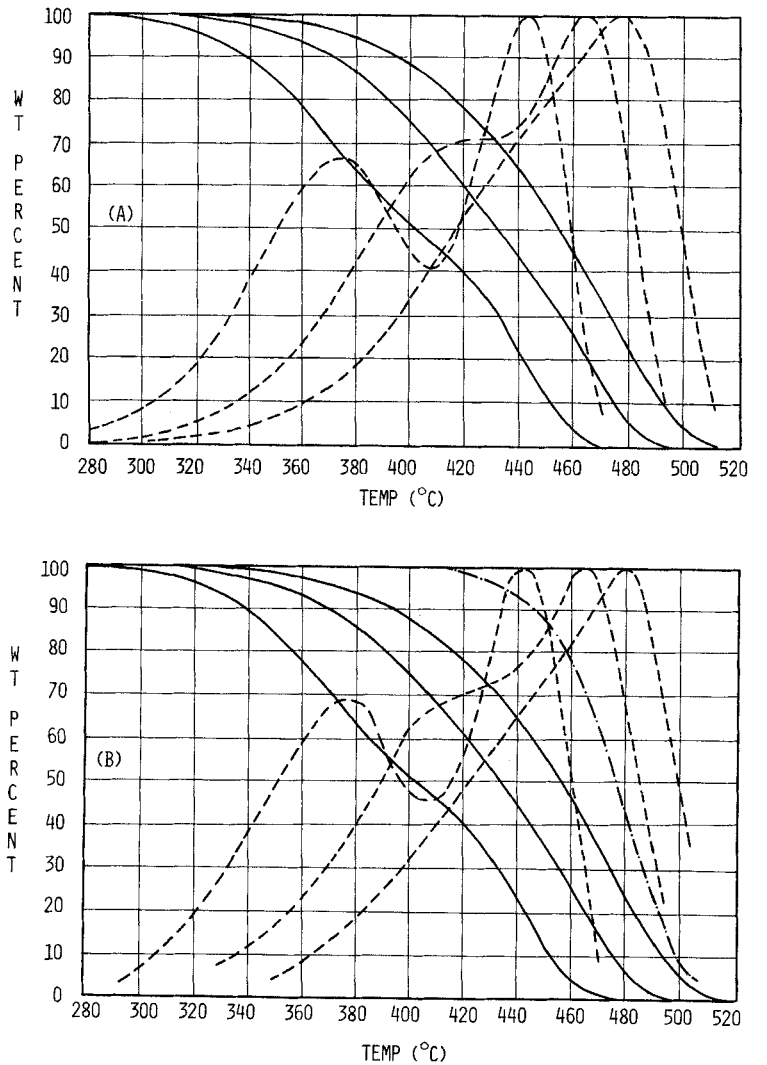

FIG. 3. Theoretical TG and DTG curves for independent (A) and consecutive reactions (B) at heating rates of 0.5, 2, and 5°C/min where A_1 and E_1 are 4.458×10^6 sec^{-1} and 30 kcal/mole; A_2 and E_2 are 10^{15} sec^{-1} and 60 kcal/mole, and n = 1 in both reactions. The (alternate) TG curve at 5°C/min for the consecutive sequence with A_2-E_2 as the first reaction is also shown (—·).

this particular example independent and consecutive reactions give similar (but marginally distinguishable) TGA curves only because the lower activation energy reaction (E = 30) was chosen for the first reaction in the consecutive sequence (see Fig. 3 for reverse sequence).

A formal interpretation of the degradative pathway comes when the curves calculated by Eqs. (4), (5), or (6) fit the experimental TGA curves at two heating rates.

Application of the Method

A review of the literature [9, 10] suggests that the first step in the thermal decomposition of our polyurethane foam is the break-up of the urethane-urea blocks leading to collapse of the cellular structure. In the second step the more stable polyol segment fragments. Since the chemical and physical changes of the initial step will influence the course of the second step, the consecutive reaction sequence seems more appropriate although the reactions are so widely separated that an independent model is also suitable.

The "reduced rate" values of the DTG curve for the first and second reaction at a = 0.75 are 1.33 and 1.04, respectively. From Table 3 these values suggest the two-dimensional diffusion mechanism (D2) for the first reaction and a random nucleation mechanism (R, n(1/4 to 1)) for the second reaction.

Using the multiple heating rate method on the central portion of both the first and second reactions at the two heating rates gives expected E_a values of 52 and 40 kcal/mole, respectively. The slope of a plot of log $g(a)/T^2$ against 1/T for the D2 rate law gives an E_a of 52 kcal/mole for the first reaction ((E + 2RT) in the Gorbachev approximation is assumed constant). A similar plot for an R(2/3) rate law for the second reaction gives E = 37 kcal/mole—acceptably close to the multiple heating rate value of 40 kcal/mole, in view of the E_a spread expected in Table 3 to verify the suitability of an R(2/3) description. From these results we infer that the first overall step, which ends with an abrupt collapse of the foam structure, is diffusion controlled (D2 law); the resultant tarry liquid gasifies in the second overall step by a random nucleation mechanism (R(2/3) law). The kinetic data for the two reactions are summarized in Table 5.

Using these data with $X_1 = 0.65$ and the expression for the TGA weight loss (Eq. 6), we obtained the very good agreement between the experimental and calculated curves shown in Fig. 1.

If we assume, as the model suggests, that a diffusion mechanism controls the first reaction step, we may formulate the following global mechanism:

(a) $F_{(c)} \rightleftharpoons F'(P)_{(c)}$

TABLE 5

Reaction	Model	g(a)	$E\left(\frac{kcal}{mole}\right)$	A (min^{-1})
1	2-D diffusion	$(1 - a) \ln (1 - a) + a$	52	3.4×10^{19}
2	Random nucleation	$[-\ln (1 - a)]^{2/3}$	39	6.8×10^{12}

(b) $F'(P)_{(c)} \longrightarrow F'_{(c)} P_{(S)}$

(c) $F'_{(c)} P_{(S)} \longrightarrow F'_{(c)} + P(g)$

Step (a) shows the in-situ formation of fragmentation-depolymerization products. To the extent that the fragmentation forms isocyanate and hydroxyl groups, this step is somewhat reversible. Step (b) shows the diffusion of these fragments to the polymer surface followed by Step (c) the desorption of Species (P). Since desorption from a polymer surface is only rate controlling at the unusually high temperatures ($> 700°K$) obtained by superheating techniques [33], we shorten the overall mechanism to Steps (a) and (b). The overall activation energy is the sum of the heat of Step (a) and the activation energy for the diffusion Step (b); i.e., $E = \Delta H_a + E_b$. The high water content of the foam formulation (Table 1) means that most of the bonds formed in the polymerization reaction will be ureas and the average structure will contain 6.5 TDI units per block, where block termini are urethane bonds. In thermal decomposition this average TDI unit will be liberated from the block with every 1.16 bonds broken. The heat of reaction of 2,4-TDI with s-butyl alcohol (our polyol is also secondary) to form the solid biscarbamate is -41.3 kcal/mole of TDI [30] or about -20.7 kcal per urethane (urea) bond. These authors also state that the reactions which yield considerable urea give approximately the same heat of reaction as do reactions which yield only urethane as product. Therefore, the heat necessary to liberate one TDI from the block (i.e., ΔH_a) is about 24 kcal per 1.16 urethane (urea) bonds. Subtracting this value from our experimental activation energy (52 kcal/mole) gives 28 kcal/mole for E_b–the diffusion step. The activation energy for the diffusion of monomer in the depolymerization of polymethyl methacrylate varies from 20 to 38 kcal/mole depending on film thickness and the extent of cross-linking [33, 34].

Neglecting diffusion, the activation energy for Step (a) is given by the sum of ΔH_a and E_{-a}; the activation energy for the reverse of Step (a). The activation energy for the reaction of s-butyl alcohol with phenyl or tolyl (o, m, or p) isocyanate ranges from ~ 10 to 13

kcal/mole depending on the amount of alcohol in the reaction mixture [31, 32]. Assuming Step (a) is mainly depolymerization, we estimate E_a as 34 to 37 kcal/mole. While this analysis gives reasonable values for the steps involved, they are based on the not fully justified, but nevertheless useful, assumption which relates our formal mechanism to the actual chemistry [35].

ACKNOWLEDGMENTS

The authors would like to acknowledge the financial support of the National Bureau of Standards under Grant 4-9026 and the Products Research Committee. Any conclusions are those of the authors and not the sponsors.

REFERENCES

[1] F. E. Rogers, T. J. Ohlemiller, A. Kurtz, and M. Summerfield, J. Fire Flammability, 8, 5 (1978).

[2] F. E. Rogers, T. J. Ohlemiller, and M. Summerfield, J. Consumer Product Flammability, 5, 59 (1978).

[3] T. J. Ohlemiller, F. E. Rogers, A. Kurtz, J. Bellan, and M. Summerfield, Experimental and Modeling Studies of Smoldering in Flexible Polyurethanes, Princeton University, Department of Mechanical and Aerospace Engineering, Report No. AMS, 1337, July 1977.

[4] T. J. Ohlemiller and F. E. Rogers, J. Fire Flammability, 9, 489 (1978).

[5] T. J. Ohlemiller and F. E. Rogers, Smoldering Combustion Studies, Princeton University, Department of Mechanical and Aerospace Engineering, Report No. 1417, December 1978.

[6] T. J. Ohlemiller, J. Bellan, and F. E. Rogers, A Model of Smoldering Combustion Applied to Flexible Polyurethane Foams, Princeton University, Department of Mechanical and Aerospace Engineering, Report No. 1419, December 1978; also to be published in Combustion and Flame.

[7] F. E. Rogers and T. J. Ohlemiller, J. Fire Flammability, 11, 32 (1980).

[8] Details of polyurethane chemistry can be found in (a) J. H. Saunders and K. C. Frisch, Polyurethanes: Chemistry and Technology, Part I, Wiley-Interscience, New York, 1962; (b) P. F. Bruins (ed.), Polyurethane Technology, Wiley-Interscience, New York, 1969; (c) Cellular Plastics, Proceedings of a Conference, Natick, Massachusetts, National Academy of Science Publication 1462, 1967.

[9] F. D. Hileman, K. J. Voorhees, L. H. Wojcik, M. M. Birky, P. W. Ryan, and I. N. Einhorn, J. Polym. Sci., Polym. Chem. Ed., 13, 571 (1975).
[10] W. D. Woolley, Br. Polym. J., 4, 27 (1972).
[11] J. D. Ingham, N. S. Rapp, and J. Hardy, J. Polym. Sci., B-2, 675 (1964).
[12] H. H. G. Jellinek and K. Takada, J. Polym. Sci., Polym. Chem. Ed., 13, 2709 (1975).
[13] M. D. Kanakia, Ph.D. Thesis, University of Utah, 1973, University Microfilms, Ann Arbor, Mich., No. 73-20147. See also R. W. Mickelson, Thermochim. Acta, 5, 329 (1973); R. W. Mickelson and I. N. Einhorn, Ibid., 1, 147 (1970) for affect of heating rate on kinetics.
[14] L. P. Rumao and K. C. Frisch, J. Polym. Sci., Polym. Chem. Ed., 10, 1499 (1972).
[15] M. J. Antal, Jr., H. L. Friedman, and F. E. Rogers, Combust. Sci. Technol., 21, 141 (1980).
[16] V. Sestak, V. Satava, and W. Wendlandt, Thermochim. Acta, 7, 333 (1973).
[17] W. W. Wendlandt, Thermal Methods of Analysis, 2nd ed., Wiley-Interscience, New York, 1974.
[18] R. R. Baker, Thermochim. Acta, 23, 201 (1978).
[19] A. Lucci and M. Tamanini, Ibid., 13, 147 (1975).
[20] L. Battezzati, A. Lucci, and G. Riontino, Ibid., 23, 43 (1978).
[21] J. Sestak, Thermal Analysis, Vol. 2, Proceedings of Third ICTA, Davos 1971, Birkauser Verlag, Basel, 1972, p. 3 (see also Ref. 22).
[22] J. M. Criado and M. Morales, Thermochim. Acta, 19, 305 (1977).
[23] A. W. Coats and J. Redfern, Nature (London), 208, 68 (1964).
[24] V. M. Gorbachev, J. Therm. Anal., 8, 348 (1975).
[25] M. Balarin, Ibid., 12, 169 (1977).
[26] J. M. Criado, Thermochim. Acta, 24, 186 (1978).
[27] (a) L. Reich and S. S. Stivala, Elements of Polymer Degradation, McGraw-Hill, New York, 1971. (b) J. H. Flynn and L. A. Wall, J. Res. Natl. Bur. Stand., 70A, 487 (1966).
[28] J. Zsako, J. Therm. Anal., 5, 239 (1973).
[29] R. R. A. ABou-Shaaban and A. P. Simonelli, Thermochim. Acta, 26, 67 (1978).
[30] E. G. Lovering and K. J. Laidler, Can. J. Chem., 40, 26 (1962).
[31] E. G. Lovering and K. J. Laidler, Ibid., 40, 31 (1962).
[32] E. Dyer, H. A. Taylor, S. J. Mason, and J. Samson, J. Am. Chem. Soc., 71, 4106 (1949).
[33] R. F. Chaiken, W. H. Andersen, M. K. Barsh, E. Mishuck, G. Moe and R. D. Schultz, J. Chem. Phys., 32, 141 (1960).
[34] H. H. G. Jellinek and H. Kachi, J. Polym. Sci., Part C, 23, 87 (1968).
[35] P. D. Garn, J. Therm. Anal., 13, 581 (1978).

Accepted by editor July 18, 1979
Received for publication August 17, 1979